Available online at website: https://journal.bcrec.id/index.php/bcrec

Bulletin of Chemical Reaction Engineering & Catalysis, 20 (1) 2025, 1-19

Research Article

Performance of a Batch Operation Microbial Fuel Cell (MFC) with Cobalt Micronutrient Addition Based on Kinetic Models

Sri Rachmania Juliastuti*, Fitria Nur Laily, Raden Darmawan

Department of Chemical Engineering, Institut Teknologi Sepuluh Nopember, Jl Raya ITS, 60111, Surabaya, Indonesia.

Received: 22h November 2024; Revised: 23th December 2024; Accepted: 25th December 2024
Available online: 31th December 2024; Published regularly: April 2025

Abstract

The generation of electricity via MFC is subject to alteration by the concentration of the substrate. The objective of this study was to examine the performance of MFCs using both theoretical and experimental methods to ascertain the kinetic parameters associated with the addition of cobalt, with the aim of enhancing electricity generation via MFCs. The study demonstrated the impact of varying substrate concentrations and the composition of food waste and water, with formulas 0:5, 1:4, 2:3, 3:2, 4:1, and 5:0 (w/v). The kinetics of biochemical reactions were determined by employing the Monod and Gates-Marlar equations. The Monod equations were evaluated using three distinct representation methods. The Langmuir, Lineweaver-Burk, and Eadie-Hofstee models were employed. Conversely, the electrochemical reaction rate is evaluated through the Butler-Volmer equation. The current density derived from the theoretical approach exhibited a comparable pattern to that observed in the experimental data. The maximum power density was attained at a substrate concentration of 4:1 (w/v) exceeding 25,000 mW/m². The presented model facilitated the enhancement and optimization of MFC performance. Substrate concentration and biomass concentration exert a significant influence on MFC performance, as evidenced by the analysis of variance (ANOVA) and response surface methodology (RSM).

Keywords: ANOVA; electricity; kinetic; microbial fuel cell; response surface methodology

How to Cite: Juliastuti, S. R., Laily, F. N., Darmawan, R. (2025). Performance of a Batch Operation Microbial Fuel Cell (MFC) with Cobalt Micronutrient Addition Based on Kinetic Models. *Bulletin of Chemical Reaction Engineering & Catalysis*, 20 (1), 1-19 (doi: 10.9767/bcrec.20259)

Permalink/DOI: https://doi.org/10.9767/bcrec.20259

Supporting Information (SI): https://journal.bcrec.id/index.php/bcrec/article/downloadSuppFile/20259/5578

1. Introduction

Microbial fuel cells (MFCs) are devices that use organic compounds to generate electricity through the activity of microorganisms [1,2]. The generation of electricity by MFCs is contingent upon the proliferation of microorganism cells and the substrate concentration [3]. It is therefore imperative to ensure the stability of substrate concentration and microbial growth during the MFC process. Typically, the generation of electricity by MFCs is impeded by barriers to electron and cation transfer from the anode to the cathode [3]. The hindrance of transfer electron interior MFC handle is dependent upon the presence of substrate as a source of nutrition for microorganisms and as a fuel converted into electron.

Considering of these challenges, numerous researchers have endeavored to enhance the effectiveness of MFCs through various methodologies. These approaches involve modifications to the chamber setup, analyses of microscopic organisms, the utilization of various anode materials, and the optimization of operational parameters. One avenue for advancing MFC performance is to ascertain the energy yield of the MFC process and to elucidate

* Corresponding Author.
Email: juliastuti@its.ac.id (S.R. Juliastuti)

the advancement dynamic control through kinetic. Active models of MFC are based on biological processes [4]. The active parameters are typically determined by the substrate concentration, substrate rate, and microbial growth [5–8]. The active parameters of MFCs emerge from the interaction between the substrate and microorganisms [9]. These interactions also drive the utilization of the substrate by the organisms, as well as its conversion into electrons and particles.

In the context of energy response in MFCs, the Monod condition is a frequently used model. Monod conditions describe the relationship between bacterial growth rate and substrate concentration, in Equation (1) [4]:

$$\mu = \mu_{max} \frac{S}{K_S + S} \quad (1)$$

The specific growth rate (μ) is expressed in units of inverse hours, while the maximum specific growth rate (μ_{max}) is expressed in units of inverse hours [4]. The limiting substrate concentration (S) is expressed in grams per liter, and the half-saturation coefficient (K_s) is expressed in grams per liter. The Monod equation was used to determine bacterial growth based on the rate of substrate utilization.

In addition to evaluating bacterial development based on substrate utilization rate, substrate restraint can be assessed through kinetic analysis. Electricity generation decreases at various substrate concentrations [3]. Previous studies on the kinetics of reactions in MFCs have focused on deriving the kinetic equation or specifying the empirical equation of the reaction in MFCs. Utami reported that MFCs with tempeh waste substrate produced a kinetic parameter value K_s of 124 mg/L with a power density of 0.033 mW/m^2 [10]. Concurrently, other researchers have undertaken a comparative analysis of the kinetic constants derived from disparate methods. Illustrative of this is the work of Imwene K.O. was obtained the kinetic constants of the Monod model ranging from 99.57 to 99.63 mg/ L, the Andrew Haldane model of 50.09-50.18 mg/L, and the Han-Levenspiel model of 91.09-100.75 mg/L [11]. According to Mbugua was kinetic parameter values can also be determined based on regression (R^2). The Gompertz equation model was used and resulted in 0.911 and 0.962 [12].

A substantial research corpus has illuminated the kinetics of MFCs; however, the kinetic effect of utilizing food waste as substrate in MFC remains to be identified [13,14]. Furthermore, this study will provide an active explanation based on substrate concentration and general control factor, such as substrate concentration and biomass concentration. The objective of this study is to determine the kinetic parameters to expand the control generation of MFCs by employing hypothetical and test approaches. Moreover, the substrate concentration and several factor in MFC will elucidated by using the RSM method. This study was conducted in batch operation using a single-chamber MFC. The findings of this study will serve as a foundation for future advancements in MFC technology, particularly in the area of large-scale implementation.

2. Materials and Methods

2.1 Food Waste and Bacteria Prepares

Food waste was collected from many stalls around the Institut Teknologi Sepuluh Nopember in Surabaya, Indonesia. The food waste used has a composition of 60% carbohydrate, 30% protein, and 10% fat. The food waste was ground into a sludge using a blender (Philips, Netherlands) and then introduced into the mushrooms for hydrolysis. The study used three species of fungi: *Aspergillus oryzae, Aspergillus aculeatus,* and *Candida rugosa*, each of which contributes to helping break down proteins, carbohydrates, and lipids in food waste. Every chamber of the MFC used 0.5 grams of food waste. In each chamber, the composition of the food waste and water mixture was varied to 0:5, 1:4, 2:3, 3:2, 4:1, and 5:0 (w/v). After a 24-hour hydrolysis process, food waste enters the MFC chamber as a substrate.

2.2 MFC Configuration

The single-chamber MFC consisted of a chamber made of a plastic bottle (PET) with a volume of 1.5 liters. It consisted of an anode located 3 cm from the bottom of the chamber and a cathode located on the surface of the chamber. The anode and cathode were made of the same material, carbon cloth with dimensions of 5 cm in length, 2 cm in width, and 2 mm in thickness. The anode and cathode were connected to an external resistor (1000 Ω) via copper wire. These external wires were placed on a printed circuit board (PCB) to facilitate voltage and current measurements. Hydrolyzed food waste, *Shewanella oneidensis* MR-1 bacteria, Sidoarjo mud, and 7 μg/L micronutrient cobalt were present in the MFC chamber as the starting process. During the process at MFC, voltage and current were measured for 20 days.

2.3 Substrate Analysis

Substrate concentration was calculated as glucose concentration and analyzed using the 3,5-dinitrosalicylic acid (DNS) method. The concentration of pure glucose was measured using standard methods. The concentration was determined by comparing the measured substrate

with the concentration of pure glucose using spectrophotometric analysis (YOKE Uv1720 UV Vis Spectrophotometer, China).

2.4 Electricity Measurement

The output current was measured through an external resistor and measured with a digital multimeter (Tofuda DT830B, Japan). Measurements were taken daily during approximately 20 days of operation. The voltage and current were measured to show the amount of power generated. Power density can be calculated from the measured voltage and current. The power density (*P*) was calculated using the following equation:

$$P\ (\mathrm{mW/m^2}) = V\ (\mathrm{volts}) \times I\ (\mathrm{amps}) / A\ (\mathrm{m^2}) \qquad (2)$$

where P was the power density, V was the voltage, I was the current, and A was the area of the active electrode.

2.5 Kinetic Model

Several kinetic analyses have been performed to describe the dynamics of microorganisms within the system. As shown in Table 1, each dynamical model analysis accounted for different systems and functions [15]. The haldane equation is most commonly used to describe the effects of inhibition on high and low substrate concentrations. The Haldane equation was developed by Aiba *et al.* simplified. Another biokinetic model was proposed by Tessier at higher substrate conditions [3].

The Monod model equations are a widely utilized tool for the description of kinetic analyses pertaining to substrate and microbial growth in systems [16,17] . In this study, experimental data based on *Shewanella oneidensis* MR-1 and glucose as substrate concentrations during the growth phase of electrogenic bacteria were obtained from mixed cultures in microbial fuel cells (MFC). The experimental data may be subjected to curve fitting analysis in order to ascertain certain parameters. The determination of reaction rate parameters necessitates the identification of the requisite substrate concentration in the batch process. The reaction kinetic parameters can be calculated by recording the substrate concentration and time during the MFC process. Reaction rates are typically represented as a graph, with the highest asymptotes representing V_{max} and K_M. K_M is the substrate concentration at which the reaction rate is half of V_{max}. However, accurately determining the values of V_{max} and K_M is often challenging. To address this, Michaelis Menten was arranged in a line [14,18] :

Table 1. Kinetic analysis models

Function of Model	Type of Models	Specific Growth Rate
Common use / typical model	Monod	$\mu = \mu max \frac{S}{K_S + S}$
Inhibition models	Haldane	$\mu = \frac{\mu\, max\, S}{S + \left(\frac{S^2}{K_i}\right) + K_S}$
	Aiba *et al.*	$r = \frac{rmaxSe^{-\frac{S}{K_i}}}{K_S + S}$
	Tessier	$= rmax(e^{\left(\frac{-S}{K_{iE}}\right)} - e^{\left(\frac{-S}{K_S}\right)}$
	Edwards	$r = rmax(e^{\left(\frac{-S}{K_{iE}}\right)} - e^{\left(\frac{-S}{K_S}\right)}$
	Luong	$r = \frac{rmaxS\left(1 - \frac{S}{S_m}\right)^n}{K_S + S}$
	Hans-Levenspiel	$r = \frac{rmaxS\left(1 - \frac{S}{S_m}\right)^n}{K_S\left(1 - \frac{S}{S_m}\right)^m + S}$
	Moser	$\mu = \mu max \frac{S^n}{K_S + S^n}$
	Blackman	$\mu = \mu max \frac{S}{2K_S}$
	Monod-Nerst	$= qmax\ \varphi_a \left(\frac{S_d}{S_d + K_{Sd}}\right)\left(\frac{1}{1 + e^{-\frac{F\eta}{RT}}}\right)$
Multiplicative Monod		$q = qmax \frac{S}{S + K_S} \frac{S_{Mox}}{K_{SMox} + S_{Mox}}$

$$Langmuir\ Plot: \frac{C_S}{\mu} = \frac{K_M}{\mu max} + \frac{C_S}{\mu max} \quad (3)$$

$$Lineweaver - Burk\ Plot = \frac{1}{\mu} = \frac{1}{\mu max} + \frac{K_M}{\mu max}\frac{1}{C_S} \quad (4)$$

$$Eadie - Hofstee\ Plot: \mu = \mu max - K_M\frac{\mu}{C_S} \quad (5)$$

A Langmuir diagram was constructed by plotting C_s/μ to C_s. The resulting graph is a straight line with a slope of $1/\mu_{max}$ and an intercept of K_M/μ_{max}. A Lineweaver-Burk plot of $1/\mu$ versus $1/C_S$ gives the impression that a Langmuir diagram would yield a linear relationship. Lineweaver-Burk plot yields a slope of K_M/μ_{max} and an intercept of $1/\mu_{max}$. Subsequently, the Eadie-Hofstee plot was employed by plotting μ versus μ/C_S, resulting in the generation of a linear relationship with a slope of $-K_M$ and an intercept of μ_{max}. The three kinetic approaches, namely the Lineweaver-Burk, were frequently utilized since this graph depicts the independent variable of C_S and the dependent variable of μ [19]. However, the Lineweaver-Burk diagram becomes less precise at lower substrate concentrations.

2.6 Analysis of Variance (ANOVA) and Response Surface Method (RSM) Analysis

Response variables were determined using the Minitab 14 and Stat-Ease programs to identify dependent and independent variables. The variables include substrate concentration (X_1), cobalt concentration (X_2), and biomass concentration (X_3), as shown in Table 2. The independent variables are identified using the power density data harvested from the MFC system.

Before evaluating the response surface methodology, ANOVA analysis was applied to determine the response variable (Y). Minitab 14 statistical software was used to create linear models and evaluate the significance (p-value) and fit (lack of fit) of the regression model. Residual evaluation and normality assessment were also conducted to determine the utility of the model [20,21]. The data was analyzed using multiple linear regression to create an optimization model specified using the following Equation (6) [21] :

$$Y = \beta_0 + \beta_1 X_1 + \beta_2 X_2 + \beta_{11} X_{21} + \beta_{22} X_{22} + \beta_{12} X_1 X_2 + \varepsilon \quad (6)$$

Y is the estimated response variable, β_0 is the constant parameter, β_1, and β_2 are the linear parameters, β_{11}, and β_{22} are the quadratic parameters, β_{12} is the interaction, and ε is the random error. When using Minitab, the ideal surface response is a stationary point, and the optimal response values are determined by contour and surface plots. The stationary point is determined from the values of the regression coefficients in the second-order model.

3. Results and Discussion

3.1 Preparation of Food Waste for Substrate on MFC Process

In previous reports, food waste from several countries was found to consist of carbohydrates, proteins, and fats [22]. Wong reported that food waste is composed of 16.6–74.6% carbohydrates, 10.4–42.2% protein, and 7–32% fat (dry basis). The organic compounds present in food waste can be employed as a fuel source to generate energy [23]. Consequently, food waste can be utilized as a fuel or substrate for MFC processes.

However, food waste frequently retains the presence of fibers, including ash, cellulose, hemicellulose, and lignin [24]. The primary impediments to the microbial decomposition of these fibers and carbohydrates are their chemical composition and the presence of lignin and other complex carbohydrates. This property of food waste can be enhanced through the process of enzymatic hydrolysis, which facilitates the breakdown of lignin-carbohydrate, protein, and lipid bonds. Three fungal species were employed in an enzymatic hydrolysis process to convert food waste into monomers. Previous studies have demonstrated the efficacy of fungi in breaking down food waste into monomeric carbohydrates, proteins, and lipids. The fungus Aspergillus aculeatus, which produces the glucose monomer, was utilized to degrade carbohydrates and a range of fiber types [25]. *Aspergillus oryzae* uses proteins to break down into amino acid monomers, and *Candida rugosa* breaks down lipids into lipid monomers [26,27]. This facilitated the enzymatic hydrolysis of food waste used as a substrate for MFC [28]. Alternative hydrolysis methods, such as acidic hydrolysis, have been reported [29,30].

Table 2. Determination of independent variables and treatment codes in research

Variables	Max	Min
Substrate concentration	0.8	0
Cobalt concentration	10	1
Biomass concentration	0.48	0.1

However, acidic hydrolysis proved to be a more efficient method than enzymatic hydrolysis. The latter also releases toxic compounds, including formic acid, acetic acid, and levulinic acid, which are known to inhibit cell proliferation during the MFC process [31]. In comparison, enzymatic hydrolysis using fungi is less toxic and represents the optimal treatment method for food waste.

The hydrolysis process was carried out before the food waste was fed into the MFC process. The enzymatic hydrolysis process has broken down the polymers contained in food waste into monomers. The monomers can be glucose, amino acids, or fatty acids. In the MFC process, not only using *Shewanella oneidensis* MR-1 bacteria, but also using culture source bacteria from Sidoarjo sludge. In Sidoarjo sludge, there are *Acetobacter* and *Gluconobacter* that can convert glucose into low-molecular-weight organic acids, such as lactic acid, acetic acid, and pyruvic acid. Furthermore, these low molecular-weight organic acids are converted by *Shewanella oneidensis* MR-1 bacteria into electrons and other ions.

3.2 Effect of Concentration Substrate

The process at the MFC began by injecting food waste, *Shewanella oneidensis* MR-1, Sidoarjo mud, and the micronutrient cobalt into the chamber of the MFC. The majority of food waste consist of carbohydrate. Furthermore, the carbohydrate was broken down into its constituent monomers, namely, glucose. Therefore, substrate concentration could be represented by glucose concentration. This experiment was performed in six independent MFC units with varying substrate concentrations. The purpose of varying the substrate concentration was to determine the reaction rate depending on the substrate concentration. Trace glucose concentrations were used to determine the electrochemical analysis and utilization of food waste in MFC reactions.

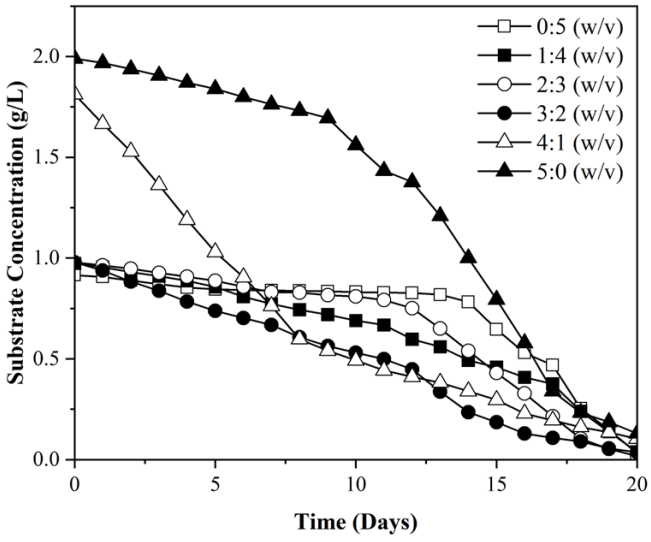

Figure 1. Substrate degradation in the MFC Process

The MFC process ran for approximately 20 days. During the process, the effect of substrate concentration was taken into account by considering different substrate concentrations (0: 5, 1: 4, 2: 3, 3: 2, 4: 1, and 5: 0 (w/v)) and bacteria kept constant at 6 billion cells/ml. The substrate concentration profile in the MFC process is shown in Figure 1. At the initial stage, the substrate concentration decreased rapidly after 12 days of operation. Although the initially released reducing glucose content increased with substrate concentration, the final sugar content was achieved at all substrate concentrations. The effect of substrate concentration on the MFC process varies from substrate to substrate [32]. Ineffective reduction of substrate concentration in the MFC process is due to the lack of electrogenic bacteria to oxidize organic compounds to electrons and cations [32].

3.3 MFC Batch Process Kinetics of Substrate and Biomass Utilization

Kinetic studies were of paramount importance in interpreting the potential MFC process, necessitating a comprehensive understanding of the interrelationship between substrate utilization, microbial growth, and biomass formation. The calculation of biological parameters may be achieved using kinetic equations, which can be applied to Michaelis-Menten diagrams or Gates-Marlar analysis. The parameters obtained using the Michaelis-Menten diagram were constructed using methods such as the Langmuir, Lineweaver-Burk, and Eadie-Hofstee models. In this study, kinetic parameters were determined and compared using the models. The results of the kinetic parameters obtained using different methods are shown in Table 1, where, μ_0 was the maximum cell growth rate and K_M was substrate concentration when the reaction rate was half of rmax, respectively. Table 1 shows that different plotting methods produced different values of μ_0 and K_M, for every different substrate load.

The effect of concentration substrate was also analyzed using MATLAB software through the Gates-Marlar Equation. By using the ODE equation in MATLAB, the graph is shown in Figure 2. Figure 2 illustrates the decline in glucose concentration and the corresponding increase in biomass concentration over time in the MFC process. Figure 2 illustrates a decline in substrate concentration concomitant with an increase in biomass concentration. This outcome demonstrates effective substrate utilization as fuel for the MFC process. The observed increase in biomass concentration provides further evidence that the MFC process was performed correctly.

Figure 2 illustrates the correlation between substrate flow rate and substrate concentration. It was determined that an increase in flow rate resulted in a corresponding decrease in substrate concentration. Consequently, the correlation between substrate flux and substrate concentration was inverse.

This condition corresponds to the following equation:

$$v_0 = \frac{F_{S0}}{C_{s0}} \quad (7)$$

Where v_0 is the volumetric flow rate with respect to the MFC process. F_{S0} is the feed rate.

3.4 The Correlation between Electricity Generation and Substrate Concentration

The power generation of MFC is contingent upon the oxidation substrate and electron transfer capacities [13]. The graph between power generation and substrate concentration demonstrated the performance of the MFC [33]. Figure 3 illustrates the impact of substrate concentration on power generation. It was discovered that the highest power generation was not consistently achieved at elevated substrate concentrations. This is due to the amount of electricity generated as a result of substrate inhibition. At the time, there was no kinetic theory available to explain this phenomenon. However, based on the kinetic analysis of substrate inhibition on electricity generation, a biodynamic rationale was applied to the nonlinear parameter fitting of the experimental data [3]. However, the experimental fitting expresses values that differ from those predicted by the kinetic inhibition theory.

As illustrated in Figure 3, food waste has been demonstrated to exert a more pronounced inhibitory effect. Figure 3 also demonstrates that the high concentration decreased at a faster rate than that of another substrate. The generation of power in the MFC commenced with the utilisation of food waste, which served to reduce the concentration of glucose and stimulate the consumption of nutrients by microorganisms. The organisms were in a state of mortality until the concentration of the substrate decreased.

3.5 Power Generation in the MFC

The maximum power generation in Figure 3 was employed to ascertain the electrochemical kinetic parameters [33]. In this investigation, the Butler-Volmer and Tafel equations were utilized to determine the kinetics of electrochemical reactions within the MFC. There are multiple methodologies for solving the Butler-Volmer and Tafel equations from an MFC performance standpoint. Theophilos presented a solution involving the combination of the Butler-Volmer equation with the Monod equation.

$$\mu = \frac{k_0.C_s}{K_m + C_s} \quad (8)$$

and Buttler-Volmer equation :

$$i = i_0[\exp\left(\alpha_a \frac{nF}{RT}(E - E_{eq})\right)] \quad (9)$$

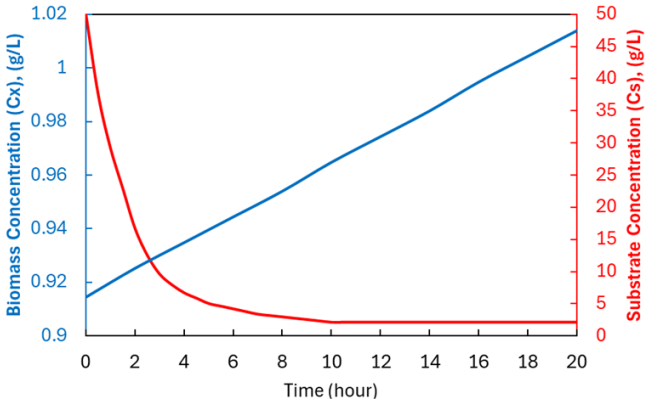

Figure 2. Correlation of substrate and biomass result from MATLAB.

Table 3. The result of the kinetic parameters

Kinetic Parameter	Plot Method	Various Substrate Loads (w/v)					
		0:5	1:4	2:3	3:2	4:1	5:0
μ_{max} (1/days)	Langmuir	1.36	2.43	0.018	0.28	1.067	1,1
	Lineweaver-Burk	0.45	0.37	0.019	0.1	0.48	0.28
	Eadie-Hofstee	0.81	3.16	0.02	0.15	1.51	0.4
	Gates-Marlar	0.012	0.02	0.02	0.007	0.37	0.002
K_M (g/L.days)	Langmuir	1.67	4.77	0.19	1,50	2.54	5.11
	Lineweaver-Burk	0.08	0.074	0.81	0.045	1.41	0.15
	Eadie-Hofstee	0.45	3.8	0.04	0.42	3.3	2.6
	Gates-Marlar	1.3	0.32	0.48	0.26	11.21	0.85

When $E - E_{eq} = \eta_a$, then Equations (8) and (9) were combined resulting in Equation (10).

$$R_1 = k_1 \frac{C_S}{K_S + C_S} exp\left(\frac{a_a F}{RT}\eta_a\right) \quad (10)$$

$$k_1 = \mu_{max} C_x \quad (11)$$

Where k_1 was the maximum specific growth rate with correlation biomass concentration (mol/(m².h)), C_s was the substrate concentration (mol/m³), K_s was the constant a half rate for substrate, a_a transfer coefficient in anode, F was Faraday constant (C/mol), R was the ideal gas constant (J/(mol. K)), T was temperature (Kelvin), and η_a was anode overpotential.

The correlation between reaction and rate was obtained by using Faraday's law :

$$R_1 = \frac{V\,I}{n\,F} \quad (12)$$

where V was the voltage of electricity (Volt), I was the current density (A/m²), n was the amount of electrons inside the reaction process, and F was the Faraday constant (C/mol).

The results obtained by calculating with 0 and parameters and the experimental current density are presented in Figure 4. The calculated current density yielded results that were found to be analogous to those observed in the experimental current density. Figure 4(a), (d), and (f) illustrate the following: For substrate

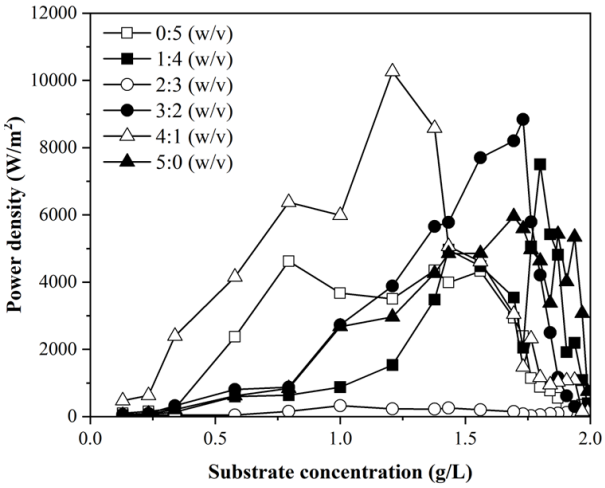

Figure 3. Effect of substrate on power density production

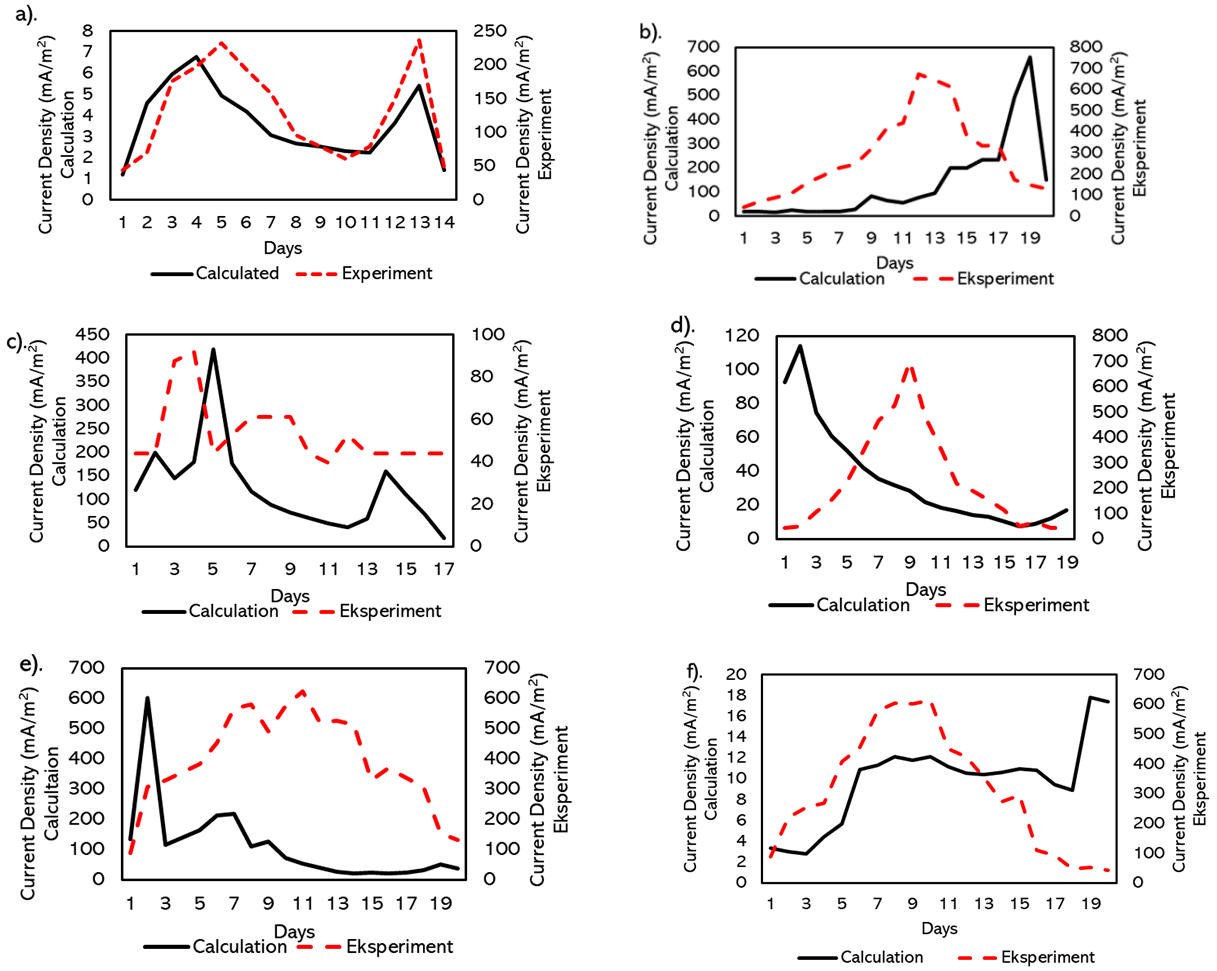

Figure 4. Comparison of calculated and experimental current density versus substrate concentration (a). 0: 5, (b). 1: 4, (c). 2: 3, (d). 3: 2, (e). 4: 1, (f). 5: 0 (w/v)

concentrations of 0.5, 3.2, and 5.0 (w/v), the calculated current density is observed to be lower than the experimentally determined current density. Therefore, the calculated current density was found to be lower than the current density obtained from the experiment. This can be attributed to the fact that the processes occurring within the experimental setup were operating at an optimal level. However, in Figures 4(b), (c), and (e), for substrates 1:4, 2:3, and 4:1 (w/v), the calculated current density is comparable to the current density obtained from the experiment. This discrepancy may be attributed to the utilization of batch operations in the present study.

3.6 Factor Influence Power Density

The RSM is an appropriate model, as evidenced by the strong correlation between experimental data and the prediction model [34–36]. To calculate the linear quadratic formula, three variables (X_1, X_2, and X_3) were analyzed using the Minitab software [37,38]. Prior to conducting the Analysis of Variance (ANOVA) test, a normality test was performed [39]. The normality test on the substrate concentration data yielded a p-value of 0.134 ($p>0.05$), thereby indicating that the data were normally distributed (Figure S1). The p-values for the normality tests on cobalt concentration, biomass concentration, and power density were 0.075, 0.377, and 0.155, respectively ($p> 0.05$) (Figure S2, S3, and S4), indicating that all data were normally distributed. The response of power density to changes in substrate, cobalt, and biomass concentrations was analyzed using an ANOVA test, yielding p-values of 0 ($p < 0.05$) for each variable (Table S1). It can therefore be concluded that this substrate can be derived. It can be concluded from these results that substrate concentration, cobalt concentration, and biomass concentration all have a significant influence on the power density response. The interaction between substrate concentration and cobalt concentration has a p-value of 0.044 ($p < 0.05$), indicating a significant difference. However, the interaction between substrate concentration and biomass concentration produces a p-value of 0.999 ($p > 0.05$), indicating no significant differences (Table S2).

The optimal conditions for achieving the maximum power density (35.9757 mW/m²) were determined through the estimation of substrate, cobalt, and biomass concentrations (1.34 mg/L, 9.7045 mg/L, and 13.0681 mg/L, respectively) (Figure S5). Figure S6 depicts a three-dimensional response surface for a fixed variable (cobalt concentration = 5.5 µg/L) with two independent variables (substrate concentration and biomass) analyzed with Minitab. As illustrated in the response surface plot, the stationary point in power density appears to be a saddle point, with the optimal power density response value attained at the maximum concentrations of both biomass and substrate. Figure S7 appears to illustrate the three-dimensional response surface for the variables substrate and cobalt concentration (with a fixed biomass concentration of 5.5 mg/L), showing that the stationary point is achieved at the greatest substrate and cobalt concentrations. Similarly, Figure S8 illustrates the optimal cobalt and biomass concentrations (at a substrate concentration of 0.5 mg/L), which yield the highest power density value. As illustrated in Figures S9-S11, the observed increase in power density is deemed appropriate, thus concluding the study and paving the way for further investigation, specifically the contour response.

Figure S12 illustrates the same concept as the surface diagram response analysis, indicating that the highest power density response can be achieved by utilizing the highest substrate, cobalt, and biomass concentrations. Additionally, a three-dimensional response surface analysis was conducted using Stat-Ease software, as depicted in Figure S12. This image presents the identical results as the Minitab analysis, but for enhanced clarity.

4. Conclusions

The findings of this study indicate that substrate and current production are correlated and enhance the performance of MFC. Across varying substrate concentrations, the highest output was observed with substrate 4:1, which achieved a power density exceeding 10,000 W/m². Model predictions based on the theoretical approach exhibited a high degree of correlation with experimental predictions. Theoretical models demonstrated a comparable trend in current density to that observed experimentally. Substrate concentration, cobalt concentration, and biomass concentration also exerted a significant influence on power density.

Acknowledgment

We are thankful to the Department of Chemical Engineering, ITS, Surabaya, for providing essential facilities to carry out our work. We are also very grateful to the Indonesian Federal Ministry of Education and Research (Kemristekdikti) for funding this project under the PMDSU Research Scholarship Program (Grant nr: 003/E5/PG.02.00/PL.PMDSU/2024).

CRedit Author Statement

Author contributions: Sri Rachmania Juliastuti: Conceptualization, Investigation, Resources, Data Curation, Review Editing, and Supervision; Fitria Nur Laily: Methodology, Formal Analysis, Data Curation, Writing Draft, Data Validation; Raden Darmawan : Conceptualization, Investigation, Review and Editing, and Supervision. All author have read and agreed to be published version of the manuscript.

References

[1] Mohd Zaini Makhtar, M., & Vadivelu, V. M. (2019). Membraneless microbial fuel cell: characterization of electrogenic bacteria and kinetic growth model. *Journal of Environmental Engineering*, 145, 5. DOI: 10.1061/(ASCE)EE.1943-7870.0001522.

[2] Xu, Z., Chen, S., Guo, S., Wan, D., Xu, H., Yan, W., ... & Feng, J. (2021). New insights in light-assisted microbial fuel cells for wastewater treatment and power generation: A win-win cooperation. *Journal of Power Sources*, 501, 230000. DOI: 10.1016/j.jpowsour.2021.230000

[3] Jafary, T., Ghoreyshi, A.A., Najafpour, G. D., Fatemi, S., & Rahimnejad, M. (2013). Investigation on performance of microbial fuel cells based on carbon sources and kinetic models. *International Journal of Energy Research*, 37(12), 1539-1549. DOI: 10.1002/er.2994

[4] Miroliaei, M.R., Samimi, A., Mohebbi-Kalhori, D., & Khorram, M. (2015). Kinetics investigation of diversity cultures of E. coli and Shewanella sp., and their combined effect with mediator on MFC performance. *Journal of Industrial and Engineering Chemistry*, 25, 42-50. DOI: 10.1016/j.jiec.2014.10.011.

[5] Reimers, C.E., Stecher III, H.A., Westall, J. C., Alleau, Y., Howell, K.A., Soule, L., ... & Girguis, P.R. (2007). Substrate degradation kinetics, microbial diversity, and current efficiency of microbial fuel cells supplied with marine plankton. *Applied and Environmental Microbiology*, 73(21), 7029-7040. DOI: 10.1128/AEM.01209-07.

[6] Shihab, M.A., Dhahir, M.A., & Mohammed, H.K. (2020). Kinetic study of air bubbles-cetyltrimethylammonium bromide (CTAB) surfactant for recovering microalgae biomass in a foam flotation column. *International Journal of Technology*, 11, 440-449. DOI: 10.14716/ijtech.v11i3.3983.

[7] Satriana, S., Maulida, A., Qardhawi, R., Lubis, Y.M., Moulana, R., Mustapha, W.A. W., & Arpi, N. (2023). Study of solid-liquid extraction kinetics of oil from dried avocado (Persea Americana) flesh using hexane as a solvent. *Int. J. Technol.*, 14(5), 982-992. DOI: 10.14716/ijtech.v14i5.6370.

[8] Prasetya, A., Darmawan, R., Araujo, T.L. B., Petrus, H.T.B.M., & Setiawan, F.A. (2021). A Growth Kinetics Model for Black Soldier Fly (Hermetia illucens) Larvae. *International Journal of Technology*, 12(1). DOI: 10.14716/ijtech.v12i1.4148.

[9] Mohanakrishna, G., Al-Raoush, R.I., Abu-Reesh, I.M., & Aljaml, K. (2019). Removal of petroleum hydrocarbons and sulfates from produced water using different bioelectrochemical reactor configurations. *Science of the Total Environment*, 665, 820-827. DOI: 10.1016/j.scitotenv.2019.02.181.

[10] Utami, T., Arbianti, R., & Trisnawati, I. (2017). Performance evaluation of single-chamber microbial fuel cell with variation of external resistance. *Asian Journal Microbiol Biotechnol Environmental Science*, 19, 872-877. DOI: 10.7454/mst.v17i1.1925

[11] Imwene, K.O., Mbui, D.N., Mbugua, J.K., Kinyua, A.P., Kairigo, P.K., & Onyatta, J.O. (2021). Kinetic modelling of microbial fuel cell voltage data from market fruit wastes in Nairobi Kenya. *International Journal of Scientific Research in Chemistry*, 6 (5), 2456-8457. DOI: 10.21654/IJSRCH.2021.6

[12] Mbugua, J.K., Mbui, D.N., Waswa, A.G., & Mwaniki, J.M. (2022). Kinetic Studies and Simulation of Microbial Fuel Cells Voltage from Clostridium Spp. and *Proteus*. *Journal of Microbial Biochemical Technology*. 14, 2, 1000483 DOI: 10.35248/1948-5948.22.14.483.

[13] Pant, D., Van Bogaert, G., Diels, L., & Vanbroekhoven, K. (2010). A review of the substrates used in microbial fuel cells (MFCs) for sustainable energy production. *Bioresource Technology*, 101 (6), 1533-1543. DOI: 10.1016/j.biortech.2009.10.017.

[14] Sharma, Y., & Li, B. (2010). The variation of power generation with organic substrates in single-chamber microbial fuel cells (SCMFCs). *Bioresource Technology*, 101 (6), 1844-1850. DOI: 10.1016/j.biortech.2009.10.040.

[15] Tsipa, A., Varnava, C.K., Grenni, P., Ferrara, V., & Pietrelli, A. (2021). Bio-electrochemical system depollution capabilities and monitoring applications: Models, applicability, advanced bio-based concept for predicting pollutant degradation and microbial growth kinetics via gene regulation modelling. *Processes*, 9 (6), 1038. DOI: 10.3390/pr9061038

[16] Boas, J.V., Oliveira, V.B., Simões, M., & Pinto, A.M.F.R. (2022). A 1D model for a single chamber microbial fuel cell. *Chemical Engineering Research and Design*, 184, 627-636. DOI: 10.1016/j.cherd.2022.06.030.

[17] Mandal, S., Sundaramurthy, S., Arisutha, S., Rene, E.R., Lens, P.N., Zahmatkesh, S., ... & Bokhari, A. (2023). Generation of bio-energy after optimization and controlling fluctuations using various sludge activated microbial fuel cell. *Environmental Science and Pollution Research*, 30 (60), 125077-125087. DOI: 10.1007/s11356-023-26344-3.

[18] Lee, J.M. (2002). Biochemical Engineering. 2.1 ed. Washington :Prentice-Hall Inc.

[19] Kaur, P., Jana, A.K., & Jana, M.M. (2024). Immobilization of Candida rugosa lipase on optimized polyamidoamine dendrimer functionalized magnetic multiwalled carbon nanotubes for green manufacture of butyl butyrate ester. *Molecular Catalysis*, 553, 113779. DOI: 10.1016/j.mcat.2023.113779.

[20] Huang, S., Zhang, J., Zhang, H., Wang, C., Zou, C., Zhang, Y., & Zhu, G. (2024). Electric field effect of microbial fuel cells on biological reactions: A review. *International Biodeterioration & Biodegradation*, 194, 105886. DOI: 10.1016/j.ibiod.2024.105886.

[21] Aghajanzadeh, I., Ramezanianpour, A. M., Amani, A., & Habibi, A. (2024). Mixture optimization of alkali activated slag concrete containing recycled concrete aggregates and silica fume using response surface method. *Construction and Building Materials*, 425, 135928. DOI: 10.1016/j.conbuildmat.2024.135928.

[22] Selvam, A., Udayakumar, M., Banu, R.J., & Wong, J. (2021). Sustainable Food Waste Management: Resource Recovery and Treatment. *Current Developments in Biotechnology and Bioengineering*, 11-41. DOI: 10.1016/B978-0-12-819148-4.00002-6.

[23] Guo, W., Feng, J., Song, H., & Sun, J. (2014). Simultaneous bioelectricity generation and decolorization of methyl orange in a two-chambered microbial fuel cell and bacterial diversity. *Environmental Science and Pollution Research*, 21, 11531-11540. DOI:10.1007/s11356-014-3071-9.

[24] Rojas, M., Ruano, D., Orrego-Restrepo, E., & Chejne, F. (2023). Non-isothermal kinetics of cellulose, hemicellulose, and lignin degradation during cocoa bean shell pyrolysis. *Biomass and Bioenergy*, 177, 106932. DOI: 10.1016/j.biombioe.2023.106932.

[25] PWolff, P.B., Nielsen, M.L., Slot, J.C., Andersen, L.N., Petersen, L.M., Isbrandt, T., ... & Hoof, J.B. (2020). Acurin A, a novel hybrid compound, biosynthesized by individually translated PKS-and NRPS-encoding genes in Aspergillus aculeatus. *Fungal Genetics and Biology*, 139, 103378. DOI: 10.1016/j.fgb.2020.103378.

[26] Pleissner, D., Kwan, T.H., & Lin, C.S. K. (2014). Fungal hydrolysis in submerged fermentation for food waste treatment and fermentation feedstock preparation. *Bioresource Technology*, 158, 48-54. DOI: 10.1016/j.biortech.2014.01.139.

[27] De Maria, P.D., Sánchez-Montero, J.M., Sinisterra, J.V., & Alcántara, A.R. (2006). Understanding Candida rugosa lipases: an overview. *Biotechnology Advances*, 24 (2), 180-196. DOI: 10.1016/j.biotechadv.2005.09.003.

[28] Turini, C.D.S., Nogueira, R.M., Pires, E.M., & Agostini, J.D.S. (2021). Enzymatic hydrolysis of carbohydrates in by-products of processed rice. *Ciência Rural*, 51(11), e20200522. DOI: 10.1590/0103-8478cr20200522

[29] Molina-Penate, E., Sánchez, A., & Artola, A. (2022). Enzymatic hydrolysis of the organic fraction of municipal solid waste: Optimization and valorization of the solid fraction for Bacillus thuringiensis biopesticide production through solid-state fermentation. *Waste Management*, 137, 304-311. DOI: 10.1016/j.wasman.2021.11.014.

[30] Zhang, C., Kang, X., Wang, F., Tian, Y., Liu, T., Su, Y., ... & Zhang, Y. (2020). Valorization of food waste for cost-effective reducing sugar recovery in a two-stage enzymatic hydrolysis platform. *Energy*, 208, 118379. DOI: 10.1016/j.energy.2020.118379.

[31] Toif, M.E., Hidayat, M., Rochmadi, R., & Budiman, A. (2023). Heterogeneous Reaction Model for Evaluating the Kinetics of Levulinic Acid Synthesis from Pretreated Sugarcane Bagasse. *International Journal of Technology*, 14(2), 300-309. DOI: 10.14716/ijtech.v14i2.5110.

[32] Toif, M.E., Hidayat, M., Rochmadi, R., & Budiman, A. (2023). Heterogeneous Reaction Model for Evaluating the Kinetics of Levulinic Acid Synthesis from Pretreated Sugarcane Bagasse. *International Journal of Technology*, 14(2), 300-309. DOI: 10.268211585/jbiochemtech.2014.

[33] Zhang, P., Liu, J., Qu, Y., Li, D., He, W., & Feng, Y. (2018). Nanomaterials for facilitating microbial extracellular electron transfer: Recent progress and challenges. *Bioelectrochemistry*, 123, 190-200. DOI: 10.1016/j.bioelechem.2018.05.005.

[34] Zhang, P., Liu, J., Qu, Y., Li, D., He, W., & Feng, Y. (2018). Nanomaterials for facilitating microbial extracellular electron transfer: Recent progress and challenges. *Bioelectrochemistry*, 123, 190-200. DOI: 10.1016/j.tsep.2024.102453.

[35] Gao, S., Zhao, Y., Zhao, X., & Zhang, Y. (2023, November). Application of response surface method based on new strategy in structural reliability analysis. In *Structures*, 57, 105202. DOI: 10.1016/j.istruc.2023.105202

[36] Amdoun, R., Khelifi, L., Khelifi-Slaoui, M., Amroune, S., Asch, M., Assaf-Ducrocq, C., & Gontier, E. (2010). Optimization of the culture medium composition to improve the production of hyoscyamine in elicited Datura stramonium L. hairy roots using the response surface methodology (RSM). *International Journal of Molecular Sciences*, 11(11), 4726-4740. DOI: 10.3390/ijms11114726.

[37] Reji, M., & Kumar, R. (2022). Response surface methodology (RSM): An overview to analyze multivariate data. *Indian Journal Microbiology Research*, 9, 241-248. DOI: 10.18231/j.ijmr.2022.042.

[38] Igbani, S., Appah, D., & Ogoni, H. A. (2020). The application of response surface methodology in minitab 16, to identify the optimal, comfort, and adverse zones of compressive strength responses in ferrous oilwell cement sheath systems. *Int. International Journal of Engineering and Modern Technology*, 6, 20-39. DOI: 10.56201/ijemt.2020.

[39] Jorge, P., Lourenço, A., & Pereira, M.O. (2015). Data quality in biofilm high-throughput routine analysis: intralaboratory protocol adaptation and experiment reproducibility. *Journal of AOAC International*, 98(6), 1721-1727. DOI: 10.5740/jaoacint.15-066.